Role of Nitric Oxide in the Chemistry and Anticancer Activity of Etoposide (VP–16,213)

8 AUTHORS, INCLUDING:

Saurabh Chatterjee
University of South Carolina
51 PUBLICATIONS   **436** CITATIONS

SEE PROFILE

Ann G Motten
National Institute of Environmental Health Sci…
38 PUBLICATIONS   **1,045** CITATIONS

SEE PROFILE

Ashutosh Kumar
National Institute of Environmental Health Sci…
24 PUBLICATIONS   **261** CITATIONS

SEE PROFILE

Ronald P Mason
National Institute of Environmental Health Sci…
**565** PUBLICATIONS   **21,077** CITATIONS

SEE PROFILE

Role of Nitric Oxide in the Chemistry and Anticancer Activity of Etoposide (VP-16,213)

Birandra K. Sinha,*,[†] Suchandra Bhattacharjee,[†] Saurabh Chatterjee,[†,§] JinJie Jiang,[†] Ann G. Motten,[†] Ashutosh Kumar,[†] Michael Graham Espey,[‡] and Ronald P. Mason[†]

[†]Laboratory of Toxicology & Pharmacology, National Institutes of Environmental Health Sciences, Research Triangle Park, North Carolina 27709, United States

[‡]Office of the Scientific Director, NIDDK, NIH, Bethesda, Maryland, United States

ABSTRACT: Originally identified as an innate cytotoxin, nitric oxide ($^{\bullet}$NO) formation in tumors can influence chemotherapy and exacerbate cancer progression. Here, we examined the hypothesis that $^{\bullet}$NO generation contributes to cancer cell drug resistance toward the widely used anticancer drug Etoposide (VP-16). The UV−vis spectrum of VP-16 was not changed by exposure of VP-16 to $^{\bullet}$NO in aqueous buffer. In contrast, reddish-orange compound(s) characteristic of *o*-quinone- and nitroso-VP-16 were readily generated in a hydrophobic medium (chloroform) in an oxygen-dependent manner. Similar products were also formed when the VP-16 radical, generated from VP-16 and horseradish peroxidase/ H_2O_2, was exposed directly to $^{\bullet}$NO in chloroform in the presence of oxygen. Separation and spectral analysis of VP-16 reaction extracts by electron spin resonance and UV−vis indicated the generation of the phenoxy radical and the *o*-quinone of VP-16, as well as putative nitroxide, iminoxyl, and other nitrogen oxide intermediates. Nitric oxide products of VP-16 displayed significantly diminished topoisomerase II-dependent cleavage of DNA and cytotoxicity to human HL-60 leukemia cells. LPS-mediated induction of nitric oxide synthase in murine macrophages resulted in VP-16 resistance compared to Raw cells. Furthermore, $^{\bullet}$NO products derived from iNOS rapidly reacted with VP-16 leading to decreased DNA damage and cytotoxicity. Together, these observations suggest that the formation of $^{\bullet}$NO in tumors (associated macrophages) can contribute to VP-16 resistance via the detoxification of VP-16.
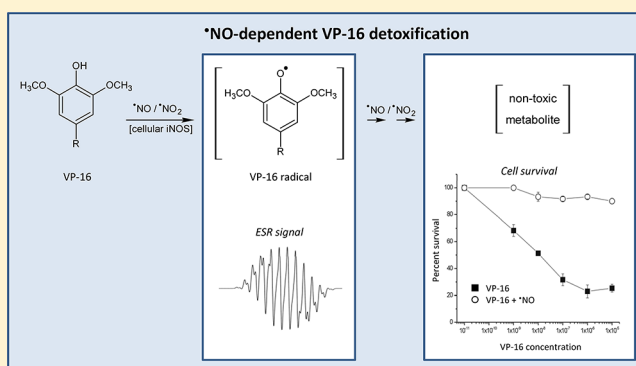
■ INTRODUCTION

The phodophyllotoxin derivative etoposide (VP-16) is one of the most active anticancer drugs for the treatment of a number of human cancers including lung and testicular cancers and lymphoma.[1] Several studies have shown that VP-16 undergoes one-electron oxidation, catalyzed by peroxidases and cytochrome P-450, to generate *o*-dihydroxy- and *o*-quinone derivatives of VP-16.[2−7] The obligatory intermediate for the formation of these metabolites is the VP-16 radical (VP-16$^{\bullet}$), formed from the oxidation of the 4′-OH group of VP-16.[2,3] Studies suggest that these metabolites are reactive and bind to cellular components[3,4] and induce DNA strand breaks through a topo II-mediated mechanism.[8,9] Furthermore, we have shown that the *o*-dihydroxy VP-16 chelates metal ions (Cu^{2+}, Fe^{3+}) to generate reactive oxygen species that induce DNA single- and double-strand breaks.[10,11] VP-16$^{\bullet}$ has been reported to cause oxidative stress both *in vitro* and *in vivo* by directly oxidizing glutathione via the glutathione thioyl radical, resulting in the formation of oxidized glutathione.[12] In addition, VP-16-*o*-quinone has been reported to form glutathione adducts in HL60 cells.[13] While several studies have indicated that the formation of dihydroxy- and *o*-quinone derivatives of VP-16

may be responsible for the development of secondary leukemia,[14−16] the role of free radical formation still remains unclear in the mechanism of action of the drug in the killing of tumor cells.

$^{\bullet}$NO and/or its products ($^{\bullet}$NO$_2$, ONOOH) have been reported to play significant roles in cancer biology, including the innate immune response, neovascularization, cancer metastasis, and cell death.[17−21] Exposure to $^{\bullet}$NO (via NO donors) modulates activities of certain anticancer drugs.[22−24] $^{\bullet}$NO or its products have also been shown to react with a wide variety of substrates including amines, thiols, and phenols.[25−28] Phenols rapidly react with $^{\bullet}$NO-derived species to form phenoxy radicals, quinones, and nitrated phenols. Thus, tyrosine, a phenolic compound and/or its phenoxyl-free radical reacts with $^{\bullet}$NO-derived species to form nitrotyrosine, and the formation of nitrotyrosine in cellular proteins has been associated with compromised protein activities.[29,30] Furthermore, $^{\bullet}$NO has been reported to react with the tyrosyl radical of

ribonucleotide reductase, resulting in the inhibition of DNA synthesis and, ultimately, cell death.[31,32]

VP-16 contains a phenolic OH group in the 4′-position, and both the cytotoxicity and the binding of VP-16 to topo II are dependent upon the presence of this moiety.[8,33,34] We hypothesized that the phenolic OH of VP-16 is susceptible to reaction with ˙NO-derived species, forming VP-16˙ and subsequently other products, thereby affecting the efficacy of VP-16-containing chemotherapy regimens. Our results support the conclusion that the intermediate nitrogen oxide chemistry of VP-16 diminishes its cytotoxic activity toward cancer cells.

■ MATERIALS AND METHODS

VP-16 was the gift of the Drug Synthesis and Chemistry Branch, Development Therapeutic Program of NCI, NIH. Supercoiled pBR322 DNA, human topoisomerase II, and SDS/KCl precipitation assay kits were obtained from Topogen, Inc., Columbus, Ohio. The NO donor compound sodium diethyl-NN(O)NO (DEANO) was obtained from Cayman Chemicals.

1400W, (N-(-aminomethyl)-benzyl)acetamidine), was purchased from Sigma Biochemical and was freshly prepared in the medium prior to use.

Stock solutions of VP-16 (10 mM) were freshly prepared in chloroform. The phenoxy radical (VP-16˙) was generated from VP-16 (1 mM) with hydrogen peroxide (0.5 mM) in the presence of horseradish peroxidase (1 mg/mL) in phosphate buffered saline (PBS) as previously described.[3] VP-16˙ was subsequently extracted in chloroform. VP-16-o-quinone was prepared by a reaction of VP-16 with sodium periodate as described by Memec,[35] and the authenticity and purity of the o-quinone were confirmed by both HPLC and mass spectrometric analysis with a molecular ion at 573 (M+1). HPLC for the analysis of the reaction products was carried out after removing the chloroform and dissolving the products in methanol as described previously,[3,4] except that a C18 column was used and MeOH–water (60:40) was the mobile phase. Under these conditions, VP-16 and VP-16-o-quinone had retention times of 2.1 and 2.7 min, respectively. Absorption spectra were recorded with a Cary UV–vis spectrophotometer (100 Bio, Varian). ESR was carried out at ambient temperature with a Bruker EMX spectrometer (Billerica, MA) equipped with an ER SHQ cavity operating at 9.80 GHz and 100 kHz modulation. Spectra were accumulated on a PC and simulated using software described previously.[36]

For aqueous reactions, ˙NO was generated from either the decomposition of DEANO in PBS, pH 7.4, or NO-saturated PBS stock solution at 25 °C. To generate the NO-PBS stock solution, ˙NO gas (National Specialty Gas, 99.5% pure) was first passed through an anaerobic KOH solution into a gastight vessel containing PBS, which was purged with argon. Stock solution of DEANO (10 mM) in 1.0 M KOH was used and was added to VP-16 solution in PBS. To generate ˙NO saturated chloroform stock solutions, ˙NO gas was first passed through an anaerobic KOH solution into a gastight vessel containing argon-purged chloroform. Chloroform was used because we found that the products formed from the reactions between VP-16 and nitric oxide were stable in chloroform for isolation and characterizations with ESR and UV–vis spectroscopy. In contrast, the reaction products in aqueous medium were either not formed (no reddish color) or were not stable for further studies and characterization. In most cases, the saturated solution of ˙NO was added to a VP-16 solution, which was also purged with argon gas and allowed to react for 5–10 min. The chloroform layer was separated, and the resulting spectrum was recorded with either ESR or UV–vis spectrophotometric analysis. For anaerobic studies with ESR, a chloroform solution of the reaction mixtures was transferred into an ESR flat cell under argon and analyzed by ESR.

Reaction products that formed following the reaction between ˙NO and VP-16 under various reaction conditions were isolated by the removal of chloroform by an argon stream and then dissolved in DMSO under argon. Cytotoxicity and DNA cleavage assays were carried out immediately following product isolation, as decomposition indicated by color change from red to yellow was evident after 12–24 h under argon at −80 °C.

DNA Cleavage Assay with pBR322. The formation of the cleavage complex in the presence of VP-16 and the products of its reaction with ˙NO/˙NO₂ were analyzed using pBR322 supercoiled DNA according to previously published methods.[37,38] Briefly, a 20 μL assay mixture contained 0.5 μg of pBR322 supercoiled DNA and an increasing concentration of drugs. The reaction was initiated by adding 5–6 units of topo II and incubating at 37 °C for 30 min. The reaction was terminated by adding 2 μL of 0.5 M EDTA and 2 μL of 10% SDS. Proteinase K (2 μL of 1 mg/mL) was added to the reaction mixture and incubated for 45 min at 50 °C. The mixture was heated to 70 °C for 1 min before loading onto 1% agarose gel for the DNA separation in Tris-acetate-EDTA buffer (pH 8.0). The DNA was stained with ethidium bromide and photographed.

Cytotoxicity Studies. The human HL-60 cells and raw 264.7 macrophage cell lines (ATCC, Rockville, Maryland) were grown in either RPMI or phenol-red free DMEM media supplemented with 10% bovine serum and antibiotics, respectively. Raw cells were used for 15 passages after which cells were discarded, and a new cell culture was started with fresh frozen stock. To induce iNOS, raw cells were treated with LPS (1 μg/mL) for 14–18 h as described previously.[39−41]

Cytotoxicity studies of products formed exogenously from the reaction of VP-16 with ˙NO/˙NO₂ were carried out with human HL60 cells (50,000) cultured in triplicate in 6-well plates in the complete RPMI media at 37 °C for 4 days. VP-16 was used for comparison, and DMSO was included with the cells. The intracellular reaction between VP-16 and endogenous ˙NO generated was examined in LPS-induced raw cells by adding various concentrations of VP-16 to the induced raw cells (1 × 10⁶), seeded in six-well plates in duplicate in the phenol-free media. Medium (100 μL) was removed at the prescribed time (4 h) and the concentration of nitrite determined by Griess reaction as previously described.[41] Cytotoxicity studies with raw cells and LPS-induced raw cells were carried out as described previously.[39] Briefly, cells (25,000−50,000/well) were plated in phenol red-free medium and treated with VP-16 for 18 h, and the cytotoxicity was measured by the MTT assay.[42] The effects of 1400W, an iNOS inhibitor,[43] on the cytotoxicity of LPS-induced raw cells were examined by pretreating raw cells with 50 uM W1400 for 2 h before inducing cells with LPS for 18 h. Cells were washed twice with ice-cold medium and suspended in the complete medium; cytotoxicity and the nitrite determinations were then carried out as described above.

SDS-KCl Precipitation Assay. The formation of covalent topo II/DNA complexes with VP-16 in raw cells (uninduced and LPS-induced) was quantitated by the SDS-KCl precipitation assay as described by Liu et al.[44] Briefly, DNA of raw cells growing in the logarithmic phase (2 × 10⁶/mL) were labeled with [methyl-3H]-thymidine (5 μci, 2 Ci/mmol; Perkin-Elmer) for 18 h. Cells were collected and washed twice with the medium, diluted in fresh medium, and seeded into a six-well plate at a density of 2.5−3.0 × 10⁵ cells/well. For the studies with the induced raw cells, cells were labeled first and then induced with LPS (1 μg/mL for 12−16 h), washed, and seeded in a six-well plate at 2.5−3.0 × 10⁵ cell/well. VP-16, dissolved in DMSO, was added and incubated for 1 h. Cells were collected by centrifugation, washed with PBS (2×), and lysed with 1 mL of prewarmed lysis solution (Topogen). After lysis and shearing of DNA, DNA-topo II-VP-16 complexes were precipitated with KCl. The precipitate was collected by centrifugation and washed extensively (four times) with the washing solution (Topogen) according to the manufacturer's instructions. The radioactivity was counted by adding 5 mL of scintillation fluid in a scintillation counter.

■ RESULTS

UV−Vis Spectrophotometer Characterization of the Reaction of VP-16 with ˙NO. The reaction of VP-16 in chloroform with ˙NO at low ˙NO to VP-16 ratios (2:1) resulted in the formation of a red product(s), which had absorption maxima of 479 and 291 nm (Figure 1B) and was significantly
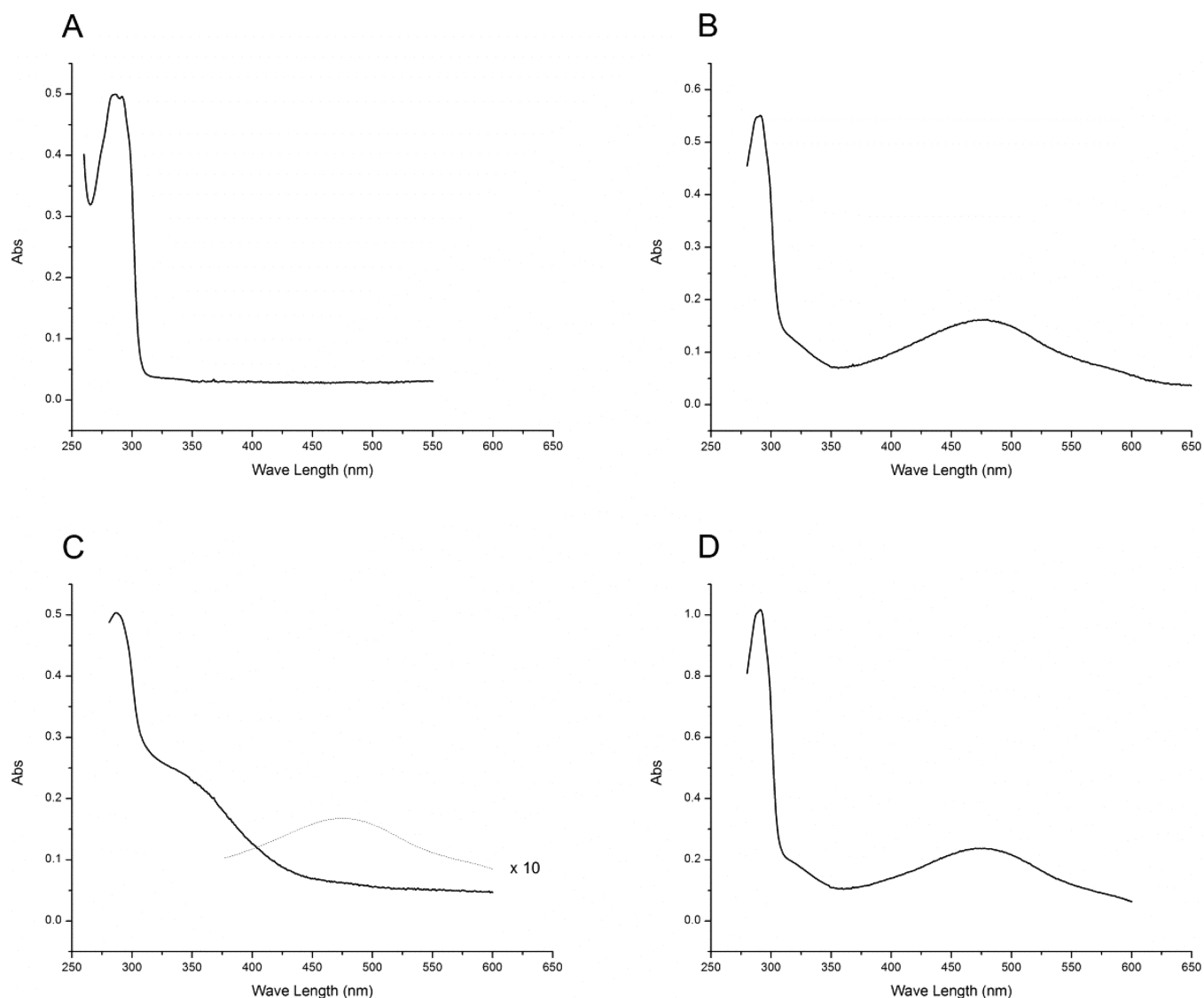
A

B

C

D

Figure 1. Absorption spectra of (A) VP-16 alone in chloroform, (B) the reactions of VP-16 with ·NO at low ·NO:VP-16 (2:1) ratio in chloroform, and (C) at high ·NO to VP-16 (5:1) ratio. The dotted line represents the spectrum recorded at a higher gain (×10) showing the presence of o-quinone at this ratio. (D) Authentic VP-16-quinone spectrum in chloroform. Following the reactions of VP-16 with ·NO/and its derived species, chloroform was removed under argon, and the products were redissolved in chloroform before recording the absorption spectrum.

different from that of the unreacted VP-16 in the same solvent (Figure 1A). When the reaction was carried out under anaerobic conditions, no products were formed, indicating that the product formation was dependent upon the presence of molecular O_2. The UV−vis spectrum of this red product was superimposable with that of the authentic VP-16-o-quinone (Figure 1D). It is of interest to note that when the reactions of ·NO with VP-16 were carried out at a high ·NO to VP-16 ratio (5:1), the formation of the red product was significantly decreased, and only a very small amount of VP-16-o-quinone was detected by UV−vis analysis at a much higher gain as shown in Figure 1C. Similar product formation was also observed when the VP-16· was reacted with ·NO gas in chloroform; the resulting absorption spectrum was identical to that obtained from a direct reaction of VP-16 with ·NO gas. This would suggest that the VP-16· is an obligatory intermediate for this ·NO-dependent product formation from VP-16.

The O_2 dependency for the formation of brick-red products in chloroform argues for ·NO₂ formed during ·NO autoxidation as the primary instigator oxidant in the formation of VP-16·. These data affirm that VP-16· once formed was subsequently vulnerable to direct reaction with ·NO or other nitrogen oxide intermediates to form the o-quinone. Furthermore, the o-quinone chromophore of VP-16 was also susceptible to further reaction with ·NO/·NO-derived species.

ESR Characterization of the Reaction of VP-16 and ·NO. To further discriminate among VP-16 intermediates generated by ·NO exposure, reaction products were examined by real-time ESR. Although not apparent in the UV−vis spectra, ESR analysis revealed that incubation of VP-16 in PBS with ·NO generated from DEANO or ·NO gas (aerobically) resulted in the formation of the previously characterized VP-16·.[8] The spectrum depicted in Figure 2a (panel A) had the following hyperfine coupling constants: $a_{OCH_3}^H = 1.33$ G; $a_{ring}^H = 1.45$ G; $a_\beta^H = 4.23$ G; $a_\gamma^H = 0.62$ and 0.39 G, respectively. A computer simulation of the radical with these coupling

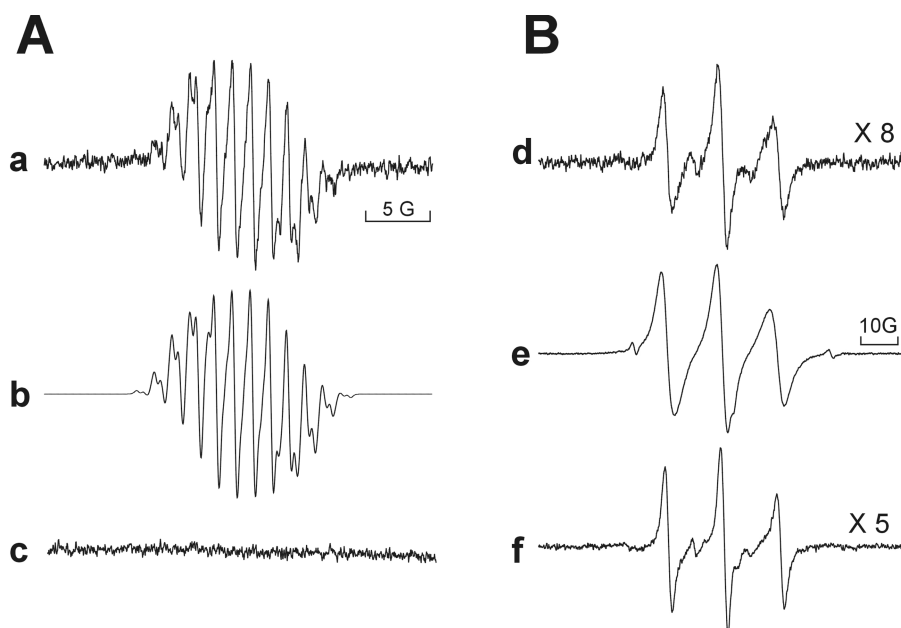**Figure 2.** Panel-A: ESR spectra of the VP-16 radical formed from (a) reaction of VP-16 (1 mM) with DEANO (1 mM) or ˙NO gas (2 mM) in PBS at pH 7.4; (b) computer simulation; and (c) spectrum recorded after 20 min. Panel B: (d) ESR spectra of radicals formed from the reaction of VP-16 (1 mM) with ˙NO/˙NO$_2$ gas in CHCl$_3$ at a low ˙NO:VP-16 ratio of 2:1 recorded after 2−3 min; (e) at a high ˙NO:VP-16 ratio (5:1); and (f) from VP-16 quinone (1 mM) and ˙NO/˙NO$_2$ (at a ratio of NO:VP-16-quinone 5:1) in CHCl$_3$. ESR spectra were recorded with a Bruker EMX operating in X-band. ESR settings were center field, 3486 G; scan range, 30 G; modulation amplitude, 1.0 G; modulation frequency 100 kHz; nominal microwave power, 21.49 mW; microwave frequency, 9.80 GHz; and receiver gain, 5 × 10^4.
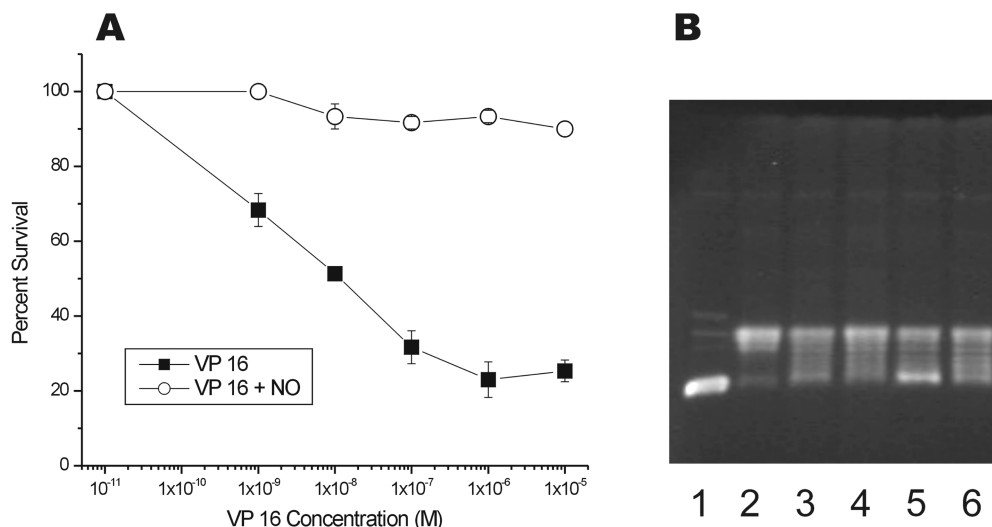

Figure 3. Panel A: Cytotoxicity of VP-16 and products formed from the reactions of ˙NO with VP-16 (5:1) in human HL-60 cells. Products (isolated as described in the Materials and Methods section) were dissolved in DMSO and added to HL60 cells (50,000 cells) and counted after 96 h. Panel B: The DNA cleavage assay with pBR322 DNA (lane 1) with topo II (lane 2) in the presence of VP-16 (25 μM and 50 μM, lanes 3 and 4) and products obtained from the reaction of VP-16 with ˙NO (5:1, 100 μM and 200 μM, lanes 5, 6). A representative DNA gel is shown here.

constants is shown in Figure 2b ($r = 0.988$). The VP-16˙ so formed, however, disappeared with time (15−20 min), indicating a quenching or a reaction of the VP-16˙ with ˙NO (Figure 2c) or other nitrogen oxides leading to ESR-silent products, consistent with the UV−vis data. Increasing concentrations of ˙NO decreased the signal intensity of the radical such that VP-16˙ became undetectable at a ratio of 2:1 (˙NO:VP-16) and above. It is also possible, however, that ˙NO reacted with O$_2$ during the ESR analysis resulting in anaerobic conditions and decreasing the formation of VP-16˙.

In contrast to the ESR spectrum obtained in aqueous medium, the deep orange/red reaction products formed consequent to either VP-16 or VP-16˙ exposure to ˙NO in chloroform yielded a complex mixture of ESR spectra, which was dependent upon the presence of molecular O$_2$, as no radicals were detected under anaerobic conditions. The ESR-detectable products had a coupling constant of $a^N = 14.8$ G, characteristic of a nitroxide radical (Figure 2d, panel B). In the presence of excess ˙NO (or when the reaction was allowed to continue for >10 min) similar radical products were formed; however, there was significant line-broadening indicating the
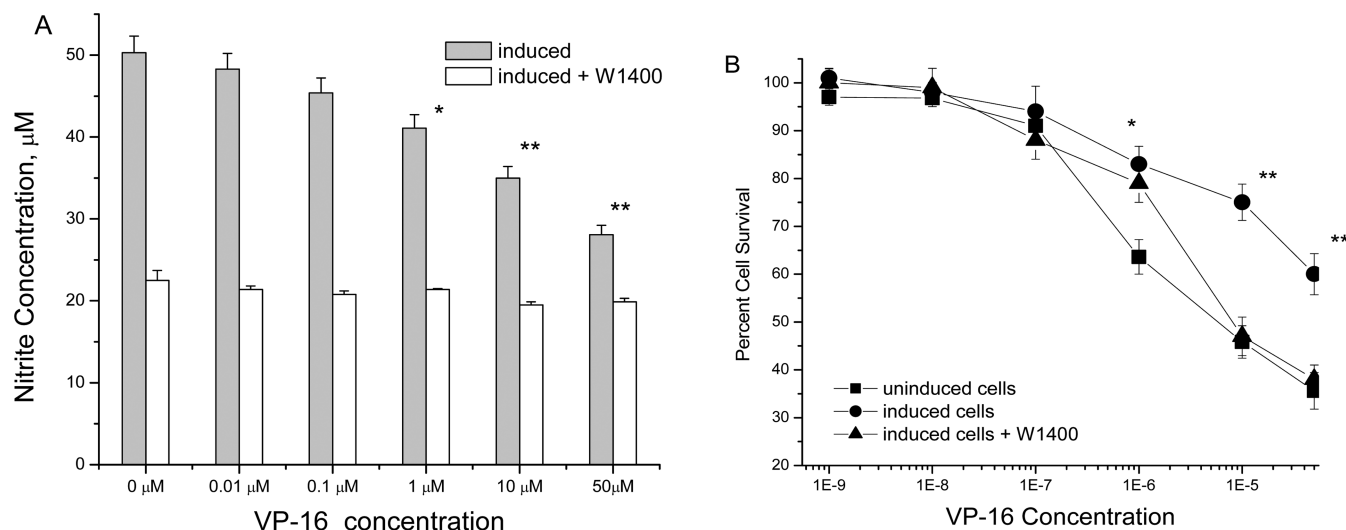
Figure 4. Panel A: The reaction of VP-16 with endogenously formed $\cdot$NO in Raw cells following treatment with LPS (1 μg/mL) for 18 h in the presence and absence of W1400 (50 μM). The induced raw cells were seeded at a density of 1×10^{6}/well in a six-well plate, and various concentrations of VP-16 were added. After 4 h of incubation, 100 μL of the media was removed, and the nitrite concentration was determined with Griess reagent. Data are the means of 3 experiments (* <0.05; ** <0.005 compared with untreated cells). The significance was determined by Student's t test. Panel B: Cytotoxicity studies with VP-16 in raw cells were carried out using the MTT assay with and without LPS induction. The effects of W1400 were examined as described in the Materials and Methods section. The cytotoxicity data are the means of 3−5 separate experiments (*< 0.05; ** <0.005 compared to uninduced cells).

presence of more nitroxide species (Figure 2e, panel B). Trace amounts were also present of two other radicals (less than 1%) that had coupling constants of a^{N} = 26 to 30 G. Large coupling constants are characteristic of iminoxyl radicals.[45]

Because our UV−vis spectrometric analysis had indicated that VP-16-o-quinone was also formed during the reaction of VP-16 with $\cdot$NO, we further examined the role of the o-quinone as an intermediate for ESR-detectable radical formation. Incubation of the VP-16 quinone with $\cdot$NO/$\cdot$NO-products resulted in ESR-detectable radical formation, and the ESR spectra were similar to those obtained previously from VP-16 and $\cdot$NO/$\cdot$NO$_2$ (Figure 2f, panel B).

Compromise of VP-16 Cytotoxicity. Since the reaction of $\cdot$NO with VP-16 results in the formation of a number of products, we determined whether this reaction may alter its cytotoxic profile toward cancer cells. In human HL-60 leukemia cells, exposure to increasing concentrations of VP-16 resulted in significant cell killing with an IC_{50} of 1×10^{-8} M (Figure 3, panel A). In contrast, cytotoxicity was decreased by several orders of magnitude (IC_{50} >10^{-5} M) when cells were exposed to VP-16-NO-derived products.

A mechanism of action of VP-16 is believed to result from the inhibition of topo II function and induction of DNA damage, resulting in both single- and double-strand breaks and ultimately in cell death. Using the purified topo II enzyme, we examined the ability of VP-16-NO-derived products to induce DNA cleavage in pBR322 DNA. Our results indicated that VP-16 was significantly (4−5-fold) more active in inducing topo II-dependent DNA cleavage than products formed from the reaction of VP-16 with $\cdot$NO (Figure 3, panel B). At lower concentrations, these products induced no DNA cleavage (data not shown) and required significantly higher concentrations of the products (e.g., 200 μM) to detect DNA cleavage (Figure 3, panel B, lane 6). These results suggest then that the reduced cytotoxicity observed against HL60 cells by VP-16 and the $\cdot$NO reaction product is related to the reduced topo II-mediated DNA cleavage.

Since the products of VP-16 reaction with $\cdot$NO/$\cdot$NO-related species in our in vitro systems were less cytotoxic to HL-60 cells and induced significantly less DNA cleavage in pBR322 DNA, we investigated whether endogenous formation of $\cdot$NO catalyzed by NOS in cells could react and affect the cytotoxicity of VP-16. To assess this, we used a mouse macrophage raw cell line, which has been shown to express iNOS and is rapidly induced by LPS to produce $\cdot$NO and $\cdot$NO-derived species.[39−41] The formation of $\cdot$NO in raw cells was confirmed in this study with the Griess reaction (control = 50.3 ± 4.0 μM nitrite; Figure 4). The results show that the presence of nitrite was significantly decreased in the presence of VP-16 (Figure 4A). The data are consistent with the reaction of $\cdot$NO/$\cdot$NO$_2$ precluding the formation of nitrite, the final product of $\cdot$NO autoxidation.[41] The cytotoxicity studies indicated that raw cells when induced to produce $\cdot$NO via iNOS become significantly resistant to killing by VP-16 (Figure 4B) as indicated by a more than 5-fold shift in IC_{50} values between the uninduced and the induced raw cells. In order to further confirm that $\cdot$NO generated from iNOS in the LPS-induced raw cells was responsible for decreasing VP-16 cytotoxicity, cytotoxicity studies were carried out in the presence of W1400, a selective inhibitor of iNOS.[43] Data presented in Figure 4 clearly show that 1400W significantly decreased nitrite production in the LPS-induced raw cells. More interestingly, 1400W completely reversed VP-16 cytotoxicity. These data are consistent with detoxification of VP-16 by $\cdot$NO/$\cdot$NO-derived species as observed in our in vitro system.

To determine whether the $\cdot$NO products derived from iNOS influences VP-16/topo II-mediated DNA damage and thus cell death, we evaluated the formation of the cleavage complexes by VP-16 in both the uninduced and the LPS-induced raw cells. As shown in Figure 5, treatment of the uninduced raw cells with VP-16 (10 μM) resulted in an increase (3-fold) in the SDS/KCl precipitate. In contrast, under similar conditions LPS-induced cells showed no significant amounts of SDS/KCl precipitate formation. At higher concentrations of VP-16, e.g.,
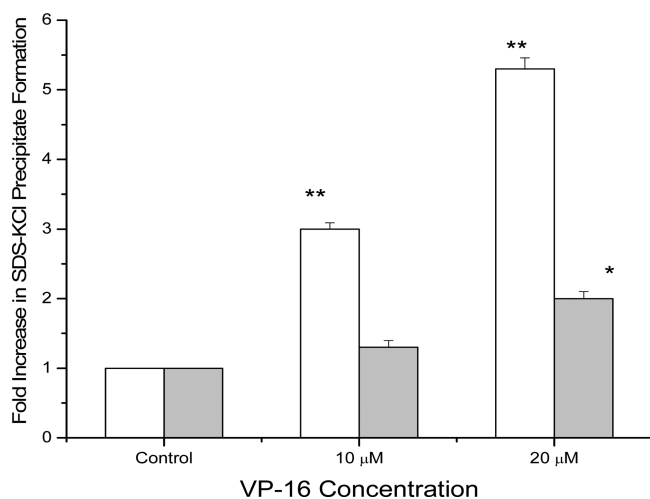
Figure 5. SDS-KCl precipitation assay with VP-16 in raw cells (□) and LPS-induced raw cells (■) as described in the Materials and Methods section. Raw cells were induced with LPS (1 μg/mL) for 14 h. Data are the means of 3 experiments (* <0.05; ** <0.005 compared with untreated control). The significance was determined by Student's t test.

20 μM VP-16, a 6-fold increase could be detected in the raw cells, while only a 2-fold increase was detected in the LPS-induced cells. These observations clearly suggest that ·NO and associated nitrogen oxides formed in the LPS-induced raw cells reacted with VP-16 rendering it less active in inducing topoisomerase II-mediated DNA damage and cytotoxicity.

■ DISCUSSION

VP-16 is used both as a single agent and in combination with other anticancer drugs for successful treatment of various cancers. Several mechanisms for the action of this drug have been proposed, including peroxidative or cytochrome P450-dependent metabolism and interactions with topo II. The role of metabolic activation to the phenoxy radical (VP-16·) and the reactive o-quinone has not been fully appreciated in the mechanism of VP-16 cytotoxicity. However, the o-quinone was found to be less cytotoxic to human breast cancer MCF-7 cells than the parent drug,[8,9] most likely due to the rapid binding of the quinone to cellular thiols, proteins, and DNA. Because of the decreased cytotoxicity of the o-quinone, this metabolism of VP-16 could be regarded as detoxification of VP-16. However, it bears mentioning that the dihydroxy derivative of VP-16 formed in cells from o-quinone by reduction chelates both Cu^{2+} and Fe^{3+} and induces significant cytotoxic DNA cleavage in the presence of H_2O_2.[10,11]

The impact of NOS activity on tumor biology is diverse and dependent on a myriad of host microenvironment factors.[46,47] Likewise, ·NO and its nitrogen oxide products can affect cancer therapy either positively or negatively.[48] The present study shows significant oxidative chemistry of ·NO with VP-16. Data from both UV−vis and ESR spectral analysis suggest that the reaction initiates through the obligate intermediacy of the 4′-phenoxy radical, with subsequent formation of o-quinone and short-lived VP-16 nitrogen oxide species. Reaction between ·NO and phenolic compounds has been the subject of numerous publications.[25−28] A key initiator in these reactions is the autoxidation of ·NO.[49,50] In the presence of molecular O_2, ·NO autoxidation results in formation of the ·NO_2 radical, which can attack the electron rich phenolic OH group to

generate the phenoxyl radical.[51,52] In this study, the formation of VP-16· and other radicals required the presence of molecular O_2, suggesting that ·NO first reacts with O_2 to generate ·NO_2 to form the VP-16 radical. Our findings suggest that once formed, VP-16· subsequently reacts with ·NO/·NO_2 to form multiple products. The ESR coupling constants (a^N = 14.0−15.0.G) for these radicals would indicate nitrogen-centered radicals, most likely nitroxide radicals. Formation of such radicals implies the addition(s) of ·NO to the VP-16·, o-quinone or activated VP-16 intermediates, e.g., quinone methides formed from the VP-16·.[3] The formation of two similar nitrogen-centered species would suggest that two different quinone methides are involved, analogous to the peroxidase metabolism of VP-16[3] and/or rearrangement of the radical species. If a nitroxide radical is formed from the addition of ·NO to the meta-positions (3′ and 5′) of the E-ring of VP-16, the two nitroxides so formed would be similar but not identical (3′- vs 5′-position) as indicated by ESR coupling constants.

Formation of nitroxide radicals is also indicated during the photolysis of DMSO or nitrosothiols/thiols in the presence of nitric oxide, resulting in three-line ESR spectra with 14−18 G splitting constants.[53] The large coupling constant (e.g., a^N = 26−30 G) observed in this study from the reaction of VP-16 with ·NO/·NO_2 would imply the formation of an iminoxyl radical. Formation of an iminoxyl radical has been suggested by Gunther et al.[45] from the trapping of nitric oxide by a tyrosyl radical (a phenoxy radical) and subsequently confirmed by direct ESR during the formation of nitrotyrosine.

It has been extensively reported that the interaction of VP-16 with topo-II causes both protein-associated DNA single- and double-strand breaks,[34,54−56] which in the absence of DNA repair results in cell death. Indeed, a significant decrease in VP-16-dependent DNA damage and cell death was observed in cell lines where the activity of topo-II had been compromised.[55,56] Our finding with HL-60 cells clearly indicates that products of VP-16 exposed to ·NO (in the presence of O_2) were no longer cytotoxic and lacked sufficient ability to induce topo II-dependent DNA cleavage in pBR322 DNA (Figure 3).

To address the relevance of this ·NO chemistry observed *in vitro*, expression of iNOS in macrophage raw 264.7 cells was utilized to directly elucidate the role of ·NO in the cytotoxicity of VP-16. Our studies clearly show that the induction of iNOS catalysis in raw cells resulted in a concomitant decrease (more than 5-fold) in VP-16 cytotoxicity compared to that of the uninduced raw cells (Figure 4B). Furthermore, the presence of VP-16 in raw macrophages resulted in a significant decrease in the formation of nitrite in the extracellular medium (Figure 4A). Studies carried out in the presence of iNOS inhibitor (1400W) further supports our conclusions that ·NO generated via the induction of NOS was responsible for significantly decreasing VP-16 activity toward LPS-induced raw cells. Together, these data indicate that endogenously formed ·NO (or ·NO-derived species) in raw cells reacted with VP-16 to generate less active metabolites of VP-16 for the significantly reduced VP-16 cytotoxicity as shown in our *in vitro* studies.

We conclude that iNOS catalysis within raw cells was sufficient to directly render the detoxification of active VP-16 via ·NO/·NO_2-dependent oxidative reactions. Microenvironmental physical chemistry influences on this iNOS-dependent detoxification process are of particular interest. ·NO will readily partition into a hydrophobic medium, such as the interior of membranes.[48] This, in combination with a relatively high rate of ·NO generation from iNOS catalysis, facilitates ·NO autox-

idation and formation of $^{\cdot}NO_2$.[49,52,56] The organic solubility of VP-16 may likewise localize and enhance interactions with the accrued maelstrom of reactive nitrogen oxides. The occurrence of both augmented iNOS catalysis[46,47] and alterations in cancer cell plasma membrane architecture (e.g., cholesterol and lipid rafts[57−59]) support a "shield" mechanism[57,59] that may predispose resistance toward VP-16 and other chemotherapeutics with similar features (e.g., teniposide).

The tumor microenvironment contains many cell types, and the most common to all tumors is the presence of inflammatory cells or macrophages.[60−62] It has been shown that the presence of macrophages in tumors is associated with tumor progression, tumor growth, and poor prognosis.[47,63] In tumors under selection pressure from chemotherapeutics, a putative shield mechanism may skew adaptation toward iNOS expression and membrane composition/dynamics that ultimately contribute to increased resistance and treatment failure. We conclude from our findings that hydrophilic lensing[50,57,59] of $^{\cdot}NO$ oxidative chemistry can detoxify VP-16 through direct nitrogen oxide radical attack. VP-16 is currently used for the treatment of a variety of cancers (e.g., lung, melanoma, and breast) known to have pronounced iNOS involvement.[21,64] From a translational viewpoint, it is tempting to suggest that the use of VP-16 and related anticancer drugs capable of reacting with $^{\cdot}NO/^{\cdot}NO_2$ may be ill-advised for patients harboring cancers with intensive iNOS- activity.

Future use of molecular and metabolomic profiling may improve clinical guidance in optimizing therapeutic choices in this regard. Further work is in progress to elucidate the role of iNOS/$^{\cdot}NO$ in the antitumor activities of other topo-active drugs.

■ AUTHOR INFORMATION

Corresponding Author
*National Institutes of Environmental Health Sciences, Research Triangle Park, North Carolina 27709. E-mail: sinha1@niehs.nih.gov.

Present Address
§S.C.: Environmental Health & Disease Laboratory, Department of Environmental Health Sciences, University of South Carolina, South Carolina.

■ ABBREVIATIONS

iNOS, inducible nitric oxide synthase; $^{\cdot}NO$, nitric oxide; $^{\cdot}NO_2$, nitrogen dioxide; VP-16, etoposide; VP-16$^{\cdot}$, VP-16-pheoxyl radical; topo II, topoisomerase II; ESR, electron spin resonance; DMSO, dimethylsulfoxide; MTT, microculture tetrazolium toxicity; PBS, phosphate buffered saline; HRP, horseradish peroxidase; LPS, bacterial lipopolysaccharide; 1400W, (N-(-aminomethyl)-benzyl)acetamidine)

■ REFERENCES

(1) Henwood, J. M., and Brogden, J. M. (1990) Etoposide. A review of its pharmacodynamic and pharmacokinetic properties, and therapeutic potentials in combination therapy of cancer. *Drugs 39*, 438−490.

(2) Haim, N., Nemec, J., Roman, J., and Sinha, B. K. (1986) Peroxidative free radical formation and o-demethylation of etoposide (VP-16) and teniposide (VM-26). *Biophys. Biochem. Res Commun. 135*, 215−220.

(3) Haim, N., Nemec, J., Roman, J., and Sinha, B. K. (1987) Peroxidase-catalyzed metabolism of etoposide (VP-16−213) and covalent binding of reactive intermediates to cellular macromolecules. *Cancer Res. 47*, 5835−5840.

(4) Haim, N., Nemec, J., Roman, J., and Sinha, B. K. (1987) In vitro metabolism of etoposide (VP-16−213) by liver microsomes and irreversible binding of reactive intermediates to microsomal proteins. *Biochem. Pharmacol. 36*, 527−536.

(5) VanMaanen, J. M. S., deVaries, J., Pappie, D., et al. (1987) Cytochrome-P-450-mediated O-demethylation- a route in the metabolic-activation of etoposide (VP-16213). *Cancer Res. 47*, 4658−4662.

(6) Kalayanaraman, B., Nemec, J., and Sinha, B. K. (1989) Characterization of free radicals produced during oxidation of etoposide (VP-16) and its catechol and quinone derivatives: an ESR study. *Biochemistry 28*, 4830−4846.

(7) Kagan, V. E., Kuzmenk, A. I., Tyurina, Y. Y., et al. (2001) Pro-oxidant and antioxidant mechanisms of etoposide in HL-60 cells: Role of myeloperoxidase. *Cancer Res. 61*, 7777−7784.

(8) Sinha, B. K., Polliti, P. M., Eliot, H. M., et al. (1990) Structure-activity relationship, cytotoxicity and topoisomerase II dependent cleavage induced by pendulum ring analogs of etoposide. *Eur. J. Cancer 26*, 590−593.

(9) Gantchev, T. G., and Hunting, D. J. (1998) The ortho-quinone metabolite of the anticancer drug etoposide (VP-16) is a potent inhibitor of the topoisomerase II-DNA cleavable complex. *Mol. Pharmacol. 53*, 422−428.

(10) Sinha, B. K., Eliot, H. M., and Kalyanaraman, B. (1988) Iron-dependent hydroxyl radical formation and DNA damage from a novel metabolite of the clinically active antitumor drug VP-16. *FEBS Lett. 227*, 240−244.

(11) Sinha, B. K., Antholine, W. M., Kalyanaraman, B., and Eliot, H. M. (1990) Copper ion-dependent oxy-radical-mediated DNA damage from dihydroxy derivative of etoposide. *Biochim. Biophys. Acta 1096*, 81−83.

(12) Katki, A. G., Kalyanaraman, B., and Sinha, B. K. (1987) Interactions of the antitumor drug, etoposide with reduced thiols in vitro and in vivo. *Chem-Biol. Interact. 62*, 237−247.

(13) Fan, Y., Schreiber, E. M., Giorgianni, A., et al. (2006) Myeloperoxidase-catalyzed metabolism of etoposide to its quinone and glutathione adduct forms in HL60 cells. *Chem. Res. Toxicol. 19*, 937−943.

(14) Felix, C. A. (2001) Leukemias related to treatment with DNA topoisomerase II inhibitors. *Med. Pediatr. Oncol. 36*, 525−535.

(15) Kagan, V. E., Yalowich, J. C., Borisenko, G. G., et al. (1999) Mechanism-based chemopreventive strategies against etoposide-induced myeloid leukemia: free radical/antioxidant approach. *Mol. Pharmacol. 56*, 494−506.

(16) Lovett, B. D., Strumberg, D., Blair, I. A., et al. (2001) Etoposide metabolite enhances topoisomerase II cleavage near leukemia-associated MLL translocation breakpoints. *Biochemistry 40*, 1159−1170.

(17) Jenkins, D. C., Charles, I. G., Thomsen, L. L., et al. (1995) Roles of nitric oxide in tumor growth. *Proc. Natl. Acad. Sci. U.S.A. 92*, 4392−96.

(18) Thomsen, L. L., Scott, J. M. J., Topley, P., et al. (1997) Selective inhibition of inducible nitric oxide synthase inhibits tumor growth in

vivo: studies with 1400W, a selective inhibitor. *Cancer Res.* 57, 3300−3304.

(19) Wink, D. A., Vodovotz, Y., Cook, J. A., et al. (1998) Role of nitric oxide chemistry in cancer treatment. *Biochemistry (Moscow)* 63, 802−809.

(20) Xu, W. M., Liu, L. Z., Loizidou, M., et al. (2002) The role of nitric oxide in cancer. *Cell Res.* 12, 311−320.

(21) Chen, G. G., Lee, T. W., Xu, H. Y., et al. (2008) Increased inducible nitric oxide synthase in lung carcinoma of smokers. *Cancer* 112, 372−381.

(22) Cook, J. A., Krishna, M. C., Pacelli, R., et al. (1997) Nitric oxide enhancement of melphalan-induced cytotoxicity. *Br. J. Cancer* 76, 325−334.

(23) Wink, D. A., Cook, J. A., Christodoulou, D., et al. (1987) Nitric oxide and some NO donor compounds enhance the cytotoxicity of cisplatin. *Nitric Oxide* 1, 88−94.

(24) Yang, D-T, Yin, J. H., Mishra, S., et al. (2002) NO-mediated chemoresistance in C6 glioma cell. *Ann. N.Y. Acad. Sci.* 962, 8−17.

(25) Wilcox, A. L., and Janzen, E. G. (1993) Nitric oxide reactions with antioxidant in model systems: sterically hindered phenols and alpha tocopherol in sodium dodecyl-sulphate (SDS) micelle. *J. Chem. Soc. Chem. Commun.* 18, 1377−1379.

(26) Janzen, E. G., Wilcox, A. L., and Manoharan, V. (1993) Reactions of nitric oxides with phenolic antioxidants and phenoxy radicals. *J. Org. Chem.* 58, 3597−3599.

(27) Cudic, M., and Ducrocq, C. (2000) Transformations of 2,6-diisopropylphenol by NO-derived nitrogen oxides, particularly peroxynitrite. *Nitric Oxide* 4, 147−156.

(28) Yenes, S., and Messeguer, A. (1999) A study of the reaction of different phenol substrate with nitric oxide and peroxynitrite. *Tetrahedron* 55, 14111−14122.

(29) Curtis, J. F., Reddy, N. G., Mason, R. P., et al. (1996) Nitric oxide: A prostaglandin H synthase 1 and 2 reducing co-substrate that does not stimulate cyclooxygenase activity or prostaglandin expression in Maurine macrophages. *Arch. Biochem. Biophys.* 335, 369−376.

(30) Chatterjee, S., Lardinois, O., Bonini, M. G., et al. (2009) Site-specific carboxypeptidase B1 tyrosine nitration and pathophysiological implications following its physical association with nitric oxide synthase-3 in experimental sepsis. *J. Immunol.* 183, 4055−4066.

(31) Sjoberg, B. M., Reichard, P., Graslund, A., and Ehrenberg, A. (1977) Nature of the free radical in ribonucleotide reductase from *Escherichia coli*. *J. Biol. Chem.* 252, 536−541.

(32) Lepoivre, M., Flaman, J. M., Bobe, P., et al. (1994) Quenching of the tyrosyl free radical of ribonucleotide reductase by nitric oxide-relationship to cytostasis induced in tumor-cell by cytotoxic macrophages. *J. Biol. Chem.* 269, 21891−21897.

(33) Loike, J. D., and Horwitz, S. B. (1976) Effects of VP-16-213 on the intracellular degradation of DNA in HeLa cells. *Biochemistry* 15, 5448−5453.

(34) Long, B. H., Musial, S. T., and Brattain, M. G. (1984) Comparison of cytotoxicity and DNA breakage of congeners of phodophyllotoxin including VP-16−213 and VM-26: a quantitative structure-activity relationship. *Biochemistry* 23, 1183−1188.

(35) Nemec J. (1986) Epipodophyllotoxinquinone Glucoside Derivatives, Method of Production and Use, US Patent 4609644.

(36) Duling, D. R. (1994) Simulation of multiple isotropic spin-trap ESR spectra. *J. Mag. Reson. Ser. B* 104, 105−110.

(37) Barrett, J. F., Gootz, T. D., McGuirk, P. R., Farrell, C. A., et al. (1989) Use of in vitro topoisomerase-II assay for studying quinolone antibacterial agents. *Antimicrob. Agents Chemother.* 33, 1697−1703.

(38) Yamazaki, H., Dilworth, A., Myers, C. E., and Sinha, B. K. (1993) Suramin inhibits DNA damage in human prostate cancer cells treated with topoisomerase inhibitors. *Prostate* 23, 25−36.

(39) Kim, H. J., Tsoyi, K., Heo, J. M., et al. (2007) Regulation of lipopolysaccharide-induced inducible nitric-oxide synthase expression through the nuclear factor kB pathway and interferon-β/tyrosine kinase 2/Janus tyrosine kinase-2 signal transducer and activator of transcription-1 signaling cascades by 2-naphthyl-6,7-dihydroxy-1,2,3,4-tetrahydroisoquinoline (THI-53), a new synthetic isoquinoline alkaloid. *JPET* 320, 782−798.

(40) Lu, S-C, Wu, H-W, Lin, Y-J, et al. (2007) The essential role of Oct-2 in LPS-induced expression of iNOS in Raw 264−7 macrophages and its regulation by trichostatin. *Am. J. Physiol. Cell Physiol.* 296, C1133−C1139.

(41) Espey, M. G., Miranda, K. M., Pluta, R. M., and Wink, D. A. (2000) Nitrosative capacity of macrophages is dependent on nitric-oxide synthase induction signals. *J. Biol. Chem.* 275, 11341−11347.

(42) Alley, M. C., Scudiero, D. A., Monks, A., et al. (1988) Feasibility of drug screening with panels of human tumor cell lines using a microculture terazolium assay. *Cancer Res.* 48, 589−601.

(43) Garvey, E. P., Oplinger, J. A., Furfine, E. S., et al. (1997) 1400W is a slow, tight binding, and highly selective inhibitor of inducible nitric-oxide synthase in vitro and in vivo. *J. Biol. Chem.* 272, 4959−4963.

(44) Liu, L. F., Rowe, T. C., Yang, L., et al. (1983) Cleavage of DNA by mammalian topoisomerase-II. *J. Biol. Chem.* 258, 15356−15371.

(45) Gunther, M. R., Sturgeon, B. E., and Mason, R. P. (2002) Nitric oxide trapping of the tyrosyl radical-chemistry and biochemistry. *Toxicology* 177, 1−9.

(46) Lancaster, J. R., and Xie, K. (2006) Tumors face NO problems? *Cancer Res.* 66, 6459−6462.

(47) Ambs, S., and Glynn, S. A. (2011) Candidate pathways linking inducible nitric oxide synthase to a basal-like transcription pattern and tumor progression in human breast cancer. *Cell Cycle* 10, 619−624.

(48) Hickok, J. R., and Thomas, D. D. (2010) Nitric oxide and cancer therapy: the emperor has NO clothes. *Curr. Pharm. Des.* 16, 381−391.

(49) Liu, X., Miller, M. J., Joshi, M. S., et al. (1998) Accelerated reactions of nitric oxide with O_2 within hydrophobic interior of biological membranes. *Proc. Natl. Acad. Sci. U.S.A.* 95, 2175−2179.

(50) Espey, M. G., Miranda, K. M., Thomas, D. D., and Wink, D. A. (2001) Distinction between nitrosating mechanisms within human cells and aqueous solutions. *J. Biol. Chem.* 276, 30085−30091.

(51) Hogg, N., Singh, R. J., Goss, S. P. A., and Kalyanaraman, B. (1996) The reaction between nitric oxide and a-tocopherol: a reappraisal. *Biochem. Biophys. Res. Commun.* 224, 696−702.

(52) Goss, S. P. A., Singh, R. J., Hogg, N., and Kalyanaraman, B. (1999) Reactions of ·NO, ·NO₂ and peroxynitrite in membranes: Physiological implications. *Free Radical Res.* 31, 597−606.

(53) Jin, J., Wu, L., and Zhang, Z. (2002) Electron paramagnetic resonance study of nitroxides generated from nitric oxide by reaction with transient radicals. *Magn. Reson. Chem.* 40, 284−288.

(54) Ross, W. E. (1985) DNA topoisomerases as targets for cancer therapy. *Biochem. Pharmacol.* 34, 4191−4195.

(55) Glisson, B., Gupta, R., Smallwood-Kentro, S., and Ross, W. E. (1986) Characterization of acquired epipodophyllotoxin resistance in Chinese-Hamster Ovary cell-line: loss of drug-stimulated DNA cleavage activity. *Cancer Res.* 46, 1934−1938.

(56) Sinha, B. K., Haim, N., Durse, L., et al. (1988) DNA strand breaks produced by etoposide (VP16−213) in sensitive and resistant human breast tumor cells: implications for the mechanism of action. *Cancer Res.* 48, 5096−6000.

(57) Moller, M. N., Li, Q., Vitturi, D. A., et al. (2007) Membrane lens effect: focusing the formation of reactive nitrogen oxides from ·NO/O₂ reactions. *Chem. Res. Toxicol.* 20, 709−714.

(58) Zhuang, L., Lin, J., Lu, M. L., et al. (2002) Cholesterol-rich lipid rafts mediate akt-regulated survival in prostate cancer cells. *Cancer Res.* 62, 2227−2231.

(59) Miersch, S., Espey, M. G., Chaube, R., et al. (2008) Plasma membrane cholesterol content affects nitric oxide diffusion dynamics and signaling. *J. Biol. Chem.* 283, 18513−18521.

(60) Lewis, C. E., and Pollard, J. W. (2006) Distinct role of macrophages in different tumor microenvironments. *Cancer Res.* 66, 605−612.

(61) Pollard, J. W. (2008) macrophages define the invasive microenvironment in breast cancer. *J. Leukocyte Biol.* 84, 623−630.

(62) Green, C. E., Liu, T., Montel, V., et al. (2009) Chemoattractant signaliing between tumor cells and macrophages regulates cancer cell migration, metastasis and neovascularization. *PLoS One 4*, 1−15.

(63) Glynn, S. A., Boersma, B. J., Dorsey, T. H., et al. (2010) Increased NOS2 predicts poor survival in estrogen receptor-negative breast cancer patients. *J. Clin Invest. 210*, 3843−3854.

(64) Grimm, E. A., Ellerhorst, J., et al. (2008) Constitutive intracellular production of iNOS and NO in human melanoma: possible role in regulation of growth and resistance to apoptosis. *Nitric Oxide 19*, 133−137.

387

dx.doi.org/10.1021/tx300480q | *Chem. Res. Toxicol.* 2013, 26, 379−387